Preparation and Characterization of Sodium Tantalate Thin Films by Hydrothermal−Electrochemical Synthesis

Yungi Lee,[†] Tomoaki Watanabe,[§] Tsuyoshi Takata,[†] Junko N. Kondo,[‡] Michikazu Hara,[‡] Masahiro Yoshimura,[§] and Kazunari Domen*[,†,||]

Department of Chemical System Engineering, The University of Tokyo, 7-3-1 Hongo, Bunkyo-ku, Tokyo, 113-8656, Japan, Chemical Resources Laboratory, Tokyo Institute of Technology, 4259 Nagatsuta, Midori-ku, Yokohama, 226-8503, Japan, Materials and Structures Lab, Tokyo Institute of Technology, 4259 Nagatsuta, Midori-ku, Yokohama, 226-8503, Japan, and Solution-Oriented Research for Science and Technology, Japan Science and Technology Co., 2-1-13 Higashiueno, Taito-ku, Tokyo 110-0015, Japan

Received January 14, 2005. Revised Manuscript Received March 1, 2005

Crystalline sodium tantalate thin films with pyrochlore ($Na_2Ta_2O_6$) and perovskite ($NaTaO_3$) structures are successfully synthesized on Ta metal substrates by a hydrothermal−electrochemical method at low temperature (≤473 K). The phase, film thickness, and domain size of the synthesized films are shown to be controllable by appropriate adjustment of the reaction conditions. Film formation mechanisms for both $Na_2Ta_2O_6$ and $NaTaO_3$ are proposed based on the experimental results.

Introduction

Hydrothermal syntheses of ceramic powders are usually carried out under moderate conditions.[1] One of the advantages of hydrothermal synthesis is the ready control of geometric properties, such as surface morphology, surface area, and particle size, by appropriate selection of starting materials and reaction conditions.

Of the various hydrothermal syntheses proposed, hydrothermal−electrochemical methods have been widely used to synthesize perovskite-type oxide thin films such as $BaTiO_3$,[2] $SrTiO_3$,[3] $BaZrO_3$,[4] $BaFeO_{3-x}$, and $LiNbO_3$.[5] By this method, perovskite-type compounds, ABO_3, are prepared on a B-site metal electrode that is anodically oxidized in an alkaline electrolyte containing A-site elements at low temperature.

A perovskite-type sodium tantalate, $NaTaO_3$, has been reported to be a highly efficient photocatalyst for overall water splitting under ultraviolet (UV) irradiation.[6] The development of thin films of semiconductor photocatalysts has attracted much attention because of the wide range of potential applications. Photocatalyst thin films solve some of the problems of powder photocatalysts, such as separation of photocatalyst from the suspension after reaction, difficulty in applying the materials in continuous flow systems, and the necessity for continuous stirring to ensure good dispersion of the powder and induce aggregation of suspended particles when present in high concentrations. Synthesized films are also applicable to photoelectrochemical systems as photoanodes[7] and are useful for characterization by electrochemical methods, which cannot be performed with photocatalyst powder.

One of the authors previously reported the successful formation of potassium tantalate thin films with pyrochlore structure by hydrothermal−electrochemical synthesis.[8,9] In this study, sodium tantalate thin films with a single phase of pyrochlore-type $Na_2Ta_2O_6$ or $NaTaO_3$ with perovskite structure were fabricated directly by the hydrothermal−electrochemical method through reaction between tantalum substrate and sodium hydroxide solution. It is the first report to prepare the perovskite-type $NaTaO_3$ thin films without any other phase. Higher alkaline concentration and higher temperatures were known to be the key factors to achieve the perovskite phase, $NaTaO_3$, for the highly active photocatalyst. The formation mechanisms for $Na_2Ta_2O_6$ and $NaTaO_3$ are also discussed.

Experimental Section

1. Preparation of Sodium Tantalate Films. A Teflon beaker containing a sodium hydroxide solution as an electrolyte was placed in an autoclave cell. The sodium hydroxide was reagent grade (>97.0%, Kanto Chemical), and its concentrations were changed from 0.5 to 5 M. Tantalum metal substrates (>99.95%, Nilaco) of 99.95% purity and dimensions of 10 × 40 × 0.2 mm were used as the working anodic electrodes. Platinum foil was employed as a counter electrode and placed in the cathode. The autoclave was sealed and heated to an appropriate temperature of 323−473 K at

* To whom correspondence should be addressed. E-mail: domen@chemsys.t.u-tokyo.ac.jp.
[†] The University of Tokyo.
[‡] Chemical Resources Laboratory, Tokyo Institute of Technology.
[§] Materials and Structures Lab., Tokyo Institute of Technology.
[||] Solution-Oriented Research for Science and Technology, Japan Science and Technology Co.

(1) Byrappa, K.; Yoshimura, M. *Handbook of hydrothermal technology − A technology for crystal growth and materials processing*; Noyes Publications: New Jersey, 2001.
(2) Yoshimura, M.; Yoo, S. E.; Hayashi, M.; Ishizawa, N. *Jpn. J. Appl. Phys.* **1989**, *28*, L2007−L2009.
(3) Yoo, S. E.; Hayashi, M.; Ogino, Y.; Ishizawa, N.; Yoshimura, M. *J. Am. Ceram. Soc.* **1990**, *73*, 2561−2563.
(4) Yoo, S. E.; Ishizawa, N.; Hayashi, M.; Yoshimura, M. *Rep. Res. Lab. Eng. Mater. Tokyo Inst. Technol.* **1991**, *No.16*, 39−53.
(5) Fuenzalida, V. M.; Pilleux, M. E. *J. Mater. Res.* **1995**, *10*, 2749−2754.
(6) Kato, H.; Kudo, A. *Catal. Lett.* **1999**, *58*, 153−155.
(7) Grätzel, M. *Nature* **2001**, *414*, 338−344.
(8) Wu, Z.; Yoshimura, M. *Thin Solid Films* **2000**, *375*, 46−50.
(9) Wu, Z. B.; Tsukada, T.; Yoshimura, M. *J. Mater. Sci.* **2000**, *35*, 2833−2839.

10.1021/cm0500859 CCC: $30.25
Published on Web 04/02/2005

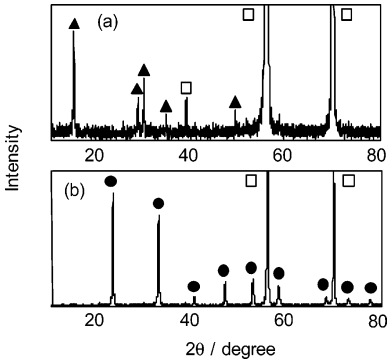

Figure 1. XRD patterns of synthesized thin films: (a) $Na_2Ta_2O_6$ prepared in 0.5 M NaOH solution, (b) $NaTaO_3$ in 5 M NaOH solution for 24 h with the current density 5 mA/cm^2 at 423K (▲, $Na_2Ta_2O_6$; ●, $NaTaO_3$; □, Ta substrate).

a heating rate of 100 K/h under saturated pressure. The reaction time, varied from 1 to 72 h, was defined as the period that the system was maintained at the specified temperature. The hydrothermal−electrochemical syntheses were carried out under galvanostatic conditions at a current density of 1−10 mA/cm^2 controlled by a potentiostat (Potentiostat/Galvanostat 2000, Toho Technical Research). Current was applied on the electrode during the reaction period (period maintained at the reaction temperature). The synthesized films were retrieved after the autoclave had cooled to room temperature. The sodium tantalate films were then washed with distilled water, ultrasonicated in ethanol, and air dried prior to characterization.

2. Characterization. The sodium tantalate films were evaluated by X-ray diffraction (XRD) analysis (RINT 2100, Rigaku) with Cu Kα radiation at 40 kV and 40 mA. The XRD patterns were collected at 2θ angles of 10−100° at a scan rate of 4°/min. Raman spectroscopy (NRS2100, Jasco) was also used to characterize the synthesized films after placement on a Ta substrate. The Raman spectra were obtained using the 514.5 or 488 nm line of an Ar ion laser. The surface morphology and thickness of the synthesized films were investigated by field-emission scanning electron microscopy (FESEM; S-4700, Hitachi), and the surfaces of the sodium tantalate films were examined by X-ray photoelectron spectroscopy (XPS; ESCA 3200, Shimadzu). All binding energies were corrected using the binding energy of Au $4f_{7/2}$ (83.8 eV).

Results and Discussion

Structural Characterization. The formation of sodium tantalate films with smooth surfaces and good adhesion to the Ta substrate was observed under a wide range of reaction conditions. The deposition of the sodium tantalate layer gave rise to multicolored films varying from green to blue and dark gray depending on the reaction conditions. Figure 1 shows typical XRD patterns for these films on Ta substrates. Parts a and b of Figure 1 indicate the formation of crystalline pyrochlore $Na_2Ta_2O_6$ and perovskite $NaTaO_3$, respectively, on the Ta metal foil. No other phases were observed, such as carbonate phases derived from CO_2 contamination in the reaction solution as observed in other films prepared by hydrothermal−electrochemical synthesis. For example, in the case of $BaTiO_3$,[10] it was very difficult to avoid barium carbonate as a contaminant.

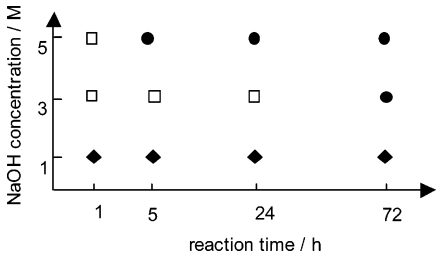

Figure 2. Diagram of the synthesized phases depending on the reaction time and NaOH concentration at 423 K with current density of 5 mA/cm^2 (●, $NaTaO_3$; □, $NaTaO_3$ + $Na_2Ta_2O_6$; ◆, $Na_2Ta_2O_6$).

The lattice parameters of the prepared sodium tantalate films were a = 10.4408 Å for $Na_2Ta_2O_6$ and 3.8823 Å for $NaTaO_3$. The former is in good agreement with the literature data,[11] whereas that for $NaTaO_3$ is somewhat smaller than the reported value,[12] possibly due to a lower density of oxygen defects in the present specimen compared to that in the reported $NaTaO_3$ powder.

It was found that the type of synthesized phase formed was strongly dependent on the reaction conditions. At temperatures below 373 K, the deposited layer was multicolored with a single phase of $Na_2Ta_2O_6$ and without impurities, regardless of the other reaction conditions. However, as the reaction temperature was increased to 423 K, the film developed as a mixture of crystalline $Na_2Ta_2O_6$ and cubic $NaTaO_3$. The intensity ratio of the peaks of the two phases ($NaTaO_3$/$Na_2Ta_2O_6$) increased with reaction temperature until $NaTaO_3$ was obtained as a single phase at 473 K (3 M NaOH solution, current density of 5 mA/cm^2). However, a single phase of $NaTaO_3$ was not obtained unless the concentration of the NaOH solution exceeded 3 M. From these results, it is obvious that the concentration of the NaOH solution and the reaction temperature are critical factors determining the phase of the synthesized films.

The phase diagram of sodium tantalate film formation is shown in Figure 2 as a function of NaOH concentration and reaction time at a reaction temperature of 423 K and a current density of 5 mA/cm^2. At a NaOH solution concentration of 1 M, all films were composed of a single phase of pyrochlore $Na_2Ta_2O_6$ regardless of the reaction time. On the other hand, the single phase of $NaTaO_3$ was obtained even at the shortest reaction time of 5 h when the reaction was performed using a high-concentration NaOH solution (5 M). In 3 M NaOH solution, the peak due to the $NaTaO_3$ phase strengthened with reaction time, and a single phase of $NaTaO_3$ was obtained after 72 h. These results demonstrate that the concentration of the NaOH solution strongly affects the phase of the synthesized films at reaction temperatures above 423 K.

To obtain a pure $NaTaO_3$ film on the Ta substrate, the reaction temperature must therefore be higher than 423 K and the concentration of the NaOH solution must be higher than 3 M. In contrast, a single phase of $Na_2Ta_2O_6$ was obtained under more moderate reaction conditions. A similar tendency has also been observed for the potassium tantalate system: Hirano et al. reported that a defect pyrochlore phase,

(10) Basca, R. R.; Rutsch, G.; Dougherty, J. P. *J. Mater. Res.* **1996**, *11*, 194−199.
(11) Michel, C.; Groult, D.; Chailleux, J. M.; Raveau, B. *Rev. Chim. Miner.* **1976**, *13*, 283−289.
(12) Ismailzade, I. G. *Kristallografiya* **1962**, *7*, 718−723.

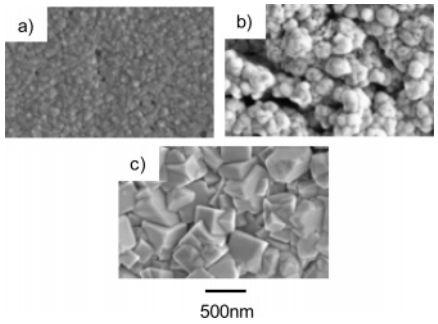

Figure 3. SEM images of surface of synthesized thin films: (a) $Na_2Ta_2O_6$ prepared in 0.5 M NaOH solution for 24 h with the current density 5 mA/cm^2 at 423 K, $NaTaO_3$ in 5 M NaOH solution for 24 h at 473 K with the current density of (b) 1 mA/cm^2 and (c) 5 mA/cm^2.

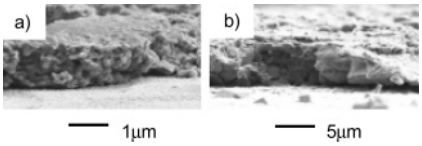

Figure 4. SEM images of cross section of synthesized thin films: (a) $Na_2Ta_2O_6$ prepared in 1 M NaOH solution for 24 h with the current density 5 mA/cm^2 at 423 K, (b) $NaTaO_3$ in 5 M NaOH solution for 24 h with the current density 5 mA/cm^2 at 473 K.

$K_2Ta_2O_6$, crystallized at 923 K, while the perovskite phase was obtained only after heating to 1123 K using alkoxide precursors.[13] It has also been reported that the pyrochlore is only an intermediate phase and that the pyrochlore reacts with KOH to form a perovskite phase in high-concentration KOH solutions.[14] Thus, the pyrochlore, $Na_2Ta_2O_6$ in this case, can be preferentially formed under moderate reaction conditions, such as lower reaction temperature, shorter reaction time, and lower NaOH concentration. Upon an increasine in the reaction temperature, reaction time, and concentration of the NaOH solution, the pyrochlore form transforms into the more stable perovskite structure, $NaTaO_3$, as confirmed in the present experiments (Figure 2).

The scanning electron micrographs of the sodium tantalate films are shown in Figure 3. The micrograph of the $Na_2Ta_2O_6$ film (Figure 3a) reveals closely packed and well-defined octahedral grains with an average grain size of 160 nm, as calculated by an intercept method. In the $NaTaO_3$ film prepared at 473 K in 5 M NaOH solution for 24 h at a current density of 1 mA/cm^2 (Figure 3b), the grains are of a uniform size (average of 200 nm) and cracks can be observed. Such cracks were not observed in the $Na_2Ta_2O_6$ film or other $NaTaO_3$ films fabricated at higher current densities. The increase in current density from 1 to 5 mA/cm^2 leads to an increase in average grain to 310 nm and the disappearance of cracks on the surface (Figure 3c).

The thickness of the films was measured from the SEM images as shown in Figure 4. The $Na_2Ta_2O_6$ film (1.2 μm thick) was substantially thinner than the $NaTaO_3$ film (3.0−4.0 μm thick; parts a and b of Figure 4). As shown in Figure 5, the thickness of the $NaTaO_3$ films increased from 2.0 to 6.0 μm with increasing current density up to 5 mA/cm^2. The

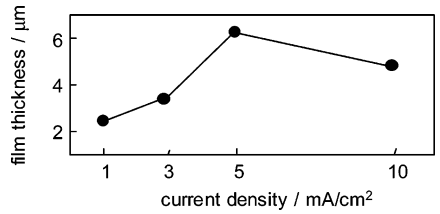

Figure 5. Change in film thickness depending on the current density for $NaTaO_3$ films.

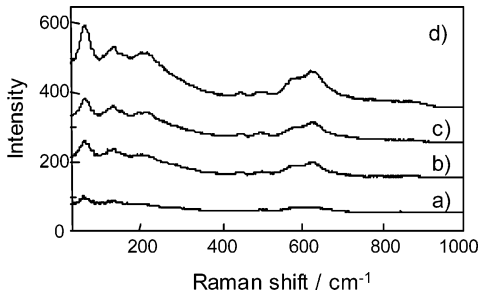

Figure 6. Raman spectra of synthesized $NaTaO_3$ thin films at 473K in 5 M NaOH solution for 24 h with the current density of (a) 1 mA/cm^2, (b) 3 mA/cm^2, (c) 5 mA/ cm^2, and (d) 10 mA/cm^2.

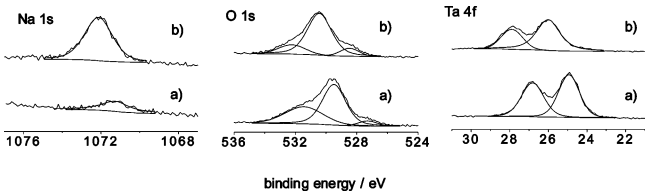

Figure 7. XPS spectra of Na 1s, O 1s, and Ta 4f peaks of (a) $Na_2Ta_2O_6$ and (b) $NaTaO_3$ thin films.

films prepared at a current density of 10 mA/ cm^2 were notably thinner, probably because the anodic dissolution rate of the Ta substrate exceeded the growth rate of the $NaTaO_3$ crystal at such high current densities. In contrast, no change in film thickness was observed for $Na_2Ta_2O_6$ film between current densities of 1 and 10 mA/cm^2.

The structure of the films was also characterized by Raman spectroscopy. Figure 6 shows the Raman spectra of the $NaTaO_3$ films prepared at various current densities. All the peaks of the synthesized films can be assigned to those reported previously for $NaTaO_3$.[15] As the current density increased, the Raman peaks became stronger, suggesting that the layer of $NaTaO_3$ phase on the Ta substrate became thicker and the grains became larger. This result is in good agreement with the direct measurement of film thickness and grain size by SEM. However, for the $Na_2Ta_2O_6$ films, no clear peaks could be observed in the Raman spectra, attributable to the low Raman activity of the $Na_2Ta_2O_6$ phase.

The narrow-scan XPS spectra of the Na1s, O1s, and Ta4f peaks for the surfaces of the $Na_2Ta_2O_6$ and $NaTaO_3$ thin films are shown in Figure 7. The Na1s peak in the $NaTaO_3$ film was observed at 1072.1 eV and is thus assignable to Na^+ cations. Ta4f$_{7/2}$ and Ta4f$_{5/2}$ peaks appeared at 25.8 and 27.8 eV, respectively, indicating the existence of Ta^{5+}. An O1s peak was also observed at 530.1 eV, presenting lattice oxygen in the $NaTaO_3$ film. From the literature data, the surface of the $NaTaO_3$ film is considered to be composed of Na^+ and

(13) Hirano, S.; Yogo, T.; Kikuta, K.; Morishita, T.; Ito, Y. *J. Am. Ceram. Soc.* **1992**, *78*, 1701.
(14) Goh, G. K. L.; Haile, S. M.; Levi, C. G.; Lange, F. F. *J. Mater. Res.* **2002**, *17*, 3168−3176.
(15) Sidorov, N. V.; Palatnikov, M. N.; NMel'nik, N. *J. Appl. Spec.* **2000**, *67*, 259−268.

Table 1. Ratio of Atomic Concentration to Ta Calculated from the Areas of XPS Spectra

	calculated amount	$Na_2Ta_2O_6$	$NaTaO_3$
Na/Ta	1.0	0.2 ± 0.1	1.0 ± 0.1
O/Ta	3.0	1.9 ± 0.1	3.0 ± 0.1

Ta^{5+} bonded to O^{2-} based on the binding energy of Na1s, O1s, and Ta4$f_{7/2}$.[16] From the atomic ratio of Ta calculated from the areas of the XPS spectra (Table 1), the experimental sodium and oxygen concentrations of the $NaTaO_3$ film are in good agreement with the calculated value for $NaTaO_3$, despite the existence of surface-adsorbed OH^-, as evidenced by the O1s peak (532.4 eV) and an uncertain peak at 528.1 eV in Figure 7b. This result shows that the $NaTaO_3$ film on the Ta substrate is well formed from the base to the upper surface. For the $Na_2Ta_2O_6$ films, the binding energies of the Na1s and O1s peaks are shifted 0.5 eV lower than those for the $NaTaO_3$ films, and the Ta4$f_{7/2}$ peak is located at a binding energy 1.0 eV lower than that for $NaTaO_3$. The atomic concentrations of sodium and lattice oxygen in the $Na_2Ta_2O_6$ film (Table 1) are low compared to the calculated values for the $Na_2Ta_2O_6$ phase. The O1s peak for the $Na_2Ta_2O_6$ film indicates a large amount of OH^- adsorbed on the surface of the $Na_2Ta_2O_6$ layer (531.8 eV), suggesting that the surface state of $Na_2Ta_2O_6$ film on the Ta substrate was somewhat hydrated during preparation by hydrothermal−electrochemical synthesis. However, the exact chemical compositions of $Na_2Ta_2O_6$ thin films are not certain. Other experiments are under going to investigate the composition of $Na_2Ta_2O_6$ thin films.

Film Formation Mechanism. Figure 8 shows the potential pH equilibrium diagram for the system of Ta and water.[17] The relative stability of Ta and Ta_2O_5 is given by

$$2Ta + 5H_2O = Ta_2O_5 + 10H^+ + 10e^-, \quad E^\circ = -0.750 - 0.0591\,(pH) \quad (1)$$

From Figure 8 and eq 1, Ta_2O_5, not Ta metal, is thermodynamically stable in the presence of water and neutral, acidic, or alkaline noncomplexing aqueous solutions. Thus, the marked activity of Ta metal toward chemical reagents is suppressed by the formation of Ta_2O_5 on the metal as a protective oxide. Ta_2O_5 is dissolved when used as an anode in a concentrated alkaline solution. Thus, if Ta_2O_5 is treated at high temperatures with alkaline oxides or carbonates, it is converted into insoluble tantalates with the general formula $MTaO_3$ (M = alkaline metal) due to a dissolution−crystallization mechanism.

It is widely accepted that the formation of ceramic films under hydrothermal−electrochemical conditions generally occurs via a dissolution−crystallization mechanism.[18,19,20] Theoretical considerations and experimental results also support the applicability of the dissolution−crystallization model as a plausible mechanism for the formation of sodium

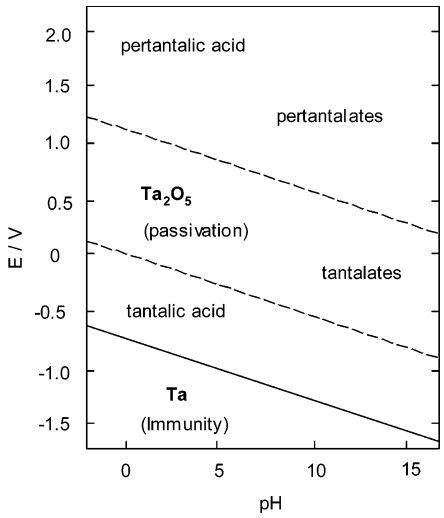

Figure 8. Potential pH equilibrium diagram for the system tantalum−water at 298 K. The words in the brackets show the theoretical domains of immunity and passivation of tantalum at 298 K.[17]

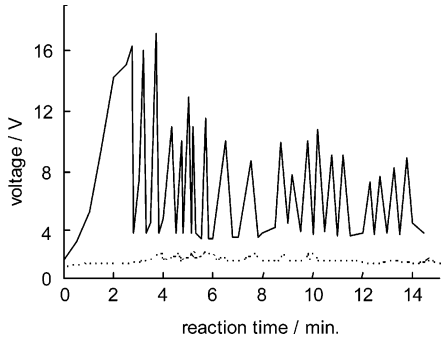

Figure 9. Plots of the voltage against the time of reaction for $Na_2Ta_2O_6$ (solid line) prepared in 1 M NaOH solution and $NaTaO_3$ (dashed line) prepared in 5 M NaOH solution at 423 K with the current density of 5 mA/cm^2.

tantalate thin films by hydrothermal−electrochemical synthesis. As described above, sodium tantalate films with a single phase of either $Na_2Ta_2O_6$ or $NaTaO_3$ can be fabricated by the hydrothermal−electrochemical method with appropriate and simple adjustment of the reaction conditions, particularly the concentration of the NaOH solution and the reaction temperature. This situation differs from that for other perovskite oxides such as potassium tantalate.

To understand these results, the change in voltage as a function of reaction time was measured during anodization of a Ta electrode, as shown in Figure 9. A large voltage fluctuation was observed for $Na_2Ta_2O_6$ (solid line) from an early stage of the reaction, presumably due to breakdown of the Ta_2O_5 film.[21,22] As mentioned above, Ta_2O_5 is thermodynamically more stable than Ta metal in solution. Thus, before applying current to the Ta substrate, a layer of Ta pentoxide or hydroxide is formed spontaneously under the hydrothermal conditions of this system. This layer then grows rapidly upon application of anodic current, as evidenced by the increase in the voltage drop in the first few minutes in

(16) Ho, S. F.; Contarini, S.; Rabalais, J. W. *J. Phys. Chem.* **1987**, *91*, 4779−1788.
(17) Pourbaix, M. *Atlas of electrochemical equilibria in aqueous solutions*; National Association of Corrosion Engineers: Houston, Texas, 1974.
(18) Yoshimura, M.; Suchanek, W. *Solid State Ionic* **1997**, *98*, 197−208.
(19) Yoshimura, M. *J. Mater. Res.* **1998**, *13*, 796−802.
(20) Yoshimura, M.; Suchanek, W.; Han, K. S. *J. Mater. Chem.* **1999**, *9*, 77−82.
(21) Bendale, P.; Vengala, S.; Amnrose, J. R.; Verink, E. D., Jr.; Adair, J. H. *J. Am. Ceram. Soc.* **1993**, *76*, 2619−2627.
(22) Parkhutik, V. P.; Albella, I. M.; Martinez-Duart, J. M. In *Electric Breakdown in anodic oxide films, Modern Aspects of Electrochemistry*; Conway, B. E., Ed.; Plenum Press: New York, 1992; Vol. 23, pp 315−389.

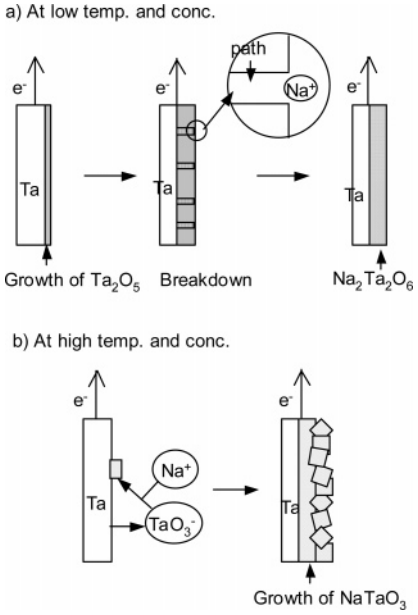

Figure 10. Mechanism of film formation for (a) $Na_2Ta_2O_6$ and (b) $NaTaO_3$ prepared by the hydrothermal−electrochemical method.

Figure 9. In contrast, the voltage during $NaTaO_3$ film formation remains almost constant (dashed line) except for a few small fluctuations.

On the basis of these experimental results, a mechanism of $Na_2Ta_2O_6$ and $NaTaO_3$ film formation is proposed, as shown in Figure 10. In this model, thin films of sodium tantalate are synthesized by anodic reaction between Ta metal and the NaOH solution. Generally, Ta_2O_5 or tantalum hydroxide is thermodynamically more stable than Ta metal in alkaline noncomplexing aqueous solutions, regardless of the concentration of the alkaline solution. However, in the present experiment, NaOH, which can drive the formation of complex oxides with Ta metal, is used as a reaction solution, and the film formation mechanism is thus more complex and dependent on the reaction conditions. The nucleation and growth of the sodium tantalate layer is affected by the nature of the Ta oxide layer and the solution chemistry. In the suggested mechanism of $Na_2Ta_2O_6$ film formation on the Ta substrate (Figure 10a), tantalum oxide/hydroxide layers are formed on the Ta metal due to the hydrothermal conditions even before anodic current is applied. After anodic current is initiated, the tantalum oxide layer grows rapidly, suppressing electrical current flow and dropping the voltage substantially, as shown in Figure 9. Dielectric breakdown of the film occurs when the voltage exceeds a critical value and is associated with the deposition of tantalum oxide layers. This behavior is consistent with the voltage fluctuation observed in Figure 9 (solid line). Breakdown of the film results in metal dissolution, oxide evolution, or oxidation of species in the electrolyte. The dissolved species then react rapidly with Na^+ ions in the vicinity of the breakdown points where temperatures locally increase sufficiently to allow reaction with Na^+. The synthesized sodium tantalate particles then cool rapidly back to the reaction temperature (423−473 K), resulting in the formation of a metastable phase of pyrochlore $Na_2Ta_2O_6$ on the Ta substrate or in the electrolyte. This formation mechanism is repeated until all tantalum oxide layers are dissolved and transformed into $Na_2Ta_2O_6$.

For $NaTaO_3$ film formation, it is also considered that a tantalum oxide layer is formed on the Ta substrate due to the hydrothermal conditions prior to current application. At high temperature and high NaOH concentration, the reactivity of the NaOH solution is sufficient to react with this preformed tantalum oxide film before the film becomes thick enough to cause dielectric breakdown, allowing the dissolution of tantalum oxide film to occur gradually. The dissolved TaO_3^- ions then react with Na^+ ions in the reaction solution to form stable $NaTaO_3$ grains on the Ta substrate by heterogeneous crystal growth. After the entire surface has been covered with small $NaTaO_3$ nuclei, the $NaTaO_3$ layers breakdown, as confirmed by the small voltage fluctuations seen in Figure 9. Such breakdown results in the dissolution of small $NaTaO_3$ grains, which recrystallize on the surface of the existing $NaTaO_3$ layer. This dissolution−recrystallization mechanism is repeated, forming successive layers of $NaTaO_3$, until the breakdown of $NaTaO_3$ layers ceases.

Conclusion

It was shown in this study to be possible to synthesize crystalline, single-phase sodium tantalate films of $Na_2Ta_2O_6$ or $NaTaO_3$ by the hydrothermal−electrochemical method at 373−473 K. The phase, film thickness, and crystallinity of the synthesized films were found to be controllable by simple adjustment of the reaction conditions. At high temperature and high concentration of the sodium hydroxide solution, cubic perovskite $NaTaO_3$ films were obtained with good adherence to the Ta substrate. At low temperature and low NaOH concentration, the pyrochlore $Na_2Ta_2O_6$ films were obtained. However, only $Na_2Ta_2O_6$ films could be synthesized from NaOH solution at concentrations below 2 M regardless of the other reaction conditions. The film thickness and average particle size were found to be influenced by the reaction time and current density applied to the Ta substrate, where longer reaction times and higher current densities produced thicker films of larger crystallites. Analysis of the voltage fluctuations during synthesis revealed remarkable differences between the formation mechanisms of the $Na_2Ta_2O_6$ and $NaTaO_3$ films, and film formation mechanisms were proposed for each of the film types on the basis of the experimental results and literature data. For the case of $Na_2Ta_2O_6$ films, the breakdown of preformed Ta_2O_5 layers results in the formation of a metastable $Na_2Ta_2O_6$ phase on the Ta substrate. In contrast, the $NaTaO_3$ thin film is obtained by repeated dissolution and recrystallization of the tantalum oxide layer, yielding a thermodynamically stable perovskite film.

Acknowledgment. This research was supported by the Solution-Oriented Research for Science and Technology program of the Japan Science and Technology Corporation.

CM0500859